IOPscience iopscience.iop.org

Home Search Collections Journals About Contact us My IOPscience

Theory of gap-node detection by angle-resolved specific heat measurement

This article has been downloaded from IOPscience. Please scroll down to see the full text article.

2005 J. Phys.: Condens. Matter 17 7971

(http://iopscience.iop.org/0953-8984/17/50/015)

View the table of contents for this issue, or go to the journal homepage for more

Download details:
IP Address: 129.252.86.83
The article was downloaded on 28/05/2010 at 07:08

Please note that terms and conditions apply.

INSTITUTE OF PHYSICS PUBLISHING JOURNAL OF PHYSICS: CONDENSED MATTER

J. Phys.: Condens. Matter **17** (2005) 7971–7980 doi:10.1088/0953-8984/17/50/015

Theory of gap-node detection by angle-resolved specific heat measurement

P Miranović[1], M Ichioka[2], K Machida[2] and N Nakai[3]

[1] Department of Physics, University of Montenegro, 81000 Podgorica, Serbia and Montenegro
[2] Department of Physics, Okayama University, Okayama 700-8530, Japan
[3] Yukawa Institute for Theoretical Physics, Kyoto University, Kyoto 606-8502, Japan

E-mail: pedjam@cg.ac.yu

Received 11 July 2005, in final form 30 September 2005
Published 2 December 2005
Online at stacks.iop.org/JPhysCM/17/7971

Abstract

The specific heat oscillation in the mixed state of type II superconductors is studied theoretically when rotating a field within a plane containing a gap minimum and maximum. The calculations are performed microscopically by solving the quasi-classical Eilenberger equation for vortex lattices. The field dependence of the oscillation amplitude can discriminate between the nodal and anisotropic gap with a finite minimum and the oscillation phase gives the gap minimum position on the Fermi surface. These also provide a way to separate out the anisotropic behaviour due to the Fermi velocity.

(Some figures in this article are in colour only in the electronic version)

1. Introduction

There has been much attention focused on exotic superconductors, including high T_c cuprates and heavy Fermion materials, in recent years. In addition to the spin structure or parity of the Cooper pair, the orbital function or the gap structure on the Fermi surface is decisive to characterize its superconductivity. These studies are expected to lead to a new pairing mechanism. Even in conventional superconductors the energy gap can vary, depending on the position on the Fermi surface. The degree of the anisotropy in the gap function is an important factor in understanding the superconductor in question. To distinguish a nodal superconductor from an anisotropic one with a finite minimum gap is of particular importance because the gap function cannot change its sign in the latter while it can in the former. Also it is crucial to determine the maximum and minimum gap positions on the Fermi surface.

It is now widely recognized that the zero-energy density of states (ZEDOS) sensitively reflects the gap structure, which is probed by a variety of experimental methods such as specific heat, thermal conductivity or scanning tunnelling spectroscopy. This is particularly true for physical quantities in the mixed state of type II superconductors. Induced vortices under an

 © 2005 IOP Publishing Ltd Printed in the UK

applied field carry a certain amount of ZEDOS around each vortex core which depends on the gap structure [1–3]. The Sommerfeld coefficient $\gamma(B)$ as a function of magnetic induction B, which is nothing but ZEDOS induced by vortices, is found to be one of the physical quantities to reveal the gap topology. In fact, there have been several $\gamma(B)$ experiments [4–9] for example on 2H-$NbSe_2$, V_3Si, Nb_3Sn or $CeRu_2$. We recently demonstrated that precise measurement $\gamma(B)$ at low field gives rise to indispensable information on the gap anisotropy [10]. In order to better characterize the gap structure it is urgent to provide further ways to analyze experimental data. For example, anisotropic behaviours in a superconductor could come from two main sources. One is the gap structure itself and the other is the Fermi velocity anisotropy due to band structure. It is often the case that these two kinds of anisotropy are mixed up and difficult to separate out individually, leading to an ambiguous conclusion for the gap structure. Thus we are required to devise some method to disentangle these two anisotropy effects.

Recently the angle-dependent specific heat experiments for the mixed state in several superconductors $LuNi_2B_2C$ [11], $CeCoIn_5$ [12] and Sr_2RuO_4 [13] have been performed to yield a characteristic oscillation pattern in $\gamma(B)$. A few per cent oscillation amplitude relative to the total in these experiments is generally consistent with the theoretical estimate [3] for nodal superconductors or strongly anisotropic gap superconductors. However, it remains open to distinguish between them. Specifically, it is reported that the oscillation amplitude becomes vanishing toward $B \to 0$ in Sr_2RuO_4 [13] while it remains a finite value in $LuNi_2B_2C$ [11] and $CeCoIn_5$ [12]. It was speculated that in the former either the gap structure has a finite minimum gap or the gap in the minor band may mask the oscillation in lower fields. Thus we need to know precise behaviour of the field-dependence of the oscillation amplitude for the two cases.

The purpose of the present paper is to examine the oscillation amplitude of the angle-dependent Sommerfeld coefficient $\gamma(B)$ when B rotates within a plane containing the gap minimum and maximum for several typical gap topologies, including line and point node superconductors and a superconductor with a finite minimum gap. We also study the oscillation behaviour of $\gamma(B)$ for the isotropic gap case with the anisotropic Fermi velocity. It turns out that this anisotropy also yields a substantial specific heat oscillation under field rotation, but we will provide information on how to distinguish it from the gap anisotropy case. The existing data of the $\gamma(B)$ oscillation experiments on $LuNi_2B_2C$, $CeCoIn_5$ and Sr_2RuO_4 are analysed in this regard. After a brief introduction to a quasi-classical framework to show how to calculate the ZEDOS for various situations, we describe the results of the ZEDOS oscillations to examine the differences between node versus nodeless gap cases in section 3 and also show the results for anisotropic Fermi velocity in section 4. Section 5 is devoted to the point node case in comparison with the line node case to supplement the above analysis. In section 6 we give a summary and discussions on the existing data. All computations are done assuming a Fermi sphere.

2. Quasi-classical theory and ZEDOS

The amplitude of the specific heat oscillations appears to be very small, just a few per cent [11–13] as mentioned before. The smallness of the effect necessitates the use of numerical solutions of Gorkov's microscopic equations of superconductivity to accurately estimate the specific heat amplitude. The quasi-classical approximation of Gorkov's equations, that we solve numerically here, is good as long as the condition $k_F\xi \gg 1$ is met. Here, k_F^{-1} is of the order of the atomic length, and ξ is the coherence length. Pairing interaction between electrons is modelled as $V(\boldsymbol{v}, \boldsymbol{v}') = V_0\Omega(\boldsymbol{v})\Omega(\boldsymbol{v}')$. This greatly simplifies the analysis, since pairing potential in this model can be written as $\Delta(\boldsymbol{r}, \boldsymbol{v}) = \Omega(\boldsymbol{v})\Psi(\boldsymbol{r})$. The orbital part of the

pairing potential, $\Omega(\boldsymbol{v})$, we simply call the gap function. The Eilenberger equations then read as ($\hbar = 1$)

$$[2\omega + \boldsymbol{v}\boldsymbol{\Pi}]f(\omega, \boldsymbol{r}, \boldsymbol{v}) = 2\Delta(\boldsymbol{r}, \boldsymbol{v})g(\omega, \boldsymbol{r}, \boldsymbol{v}), \tag{1}$$

$$[2\omega - \boldsymbol{v}\boldsymbol{\Pi}^*]f^\dagger(\omega, \boldsymbol{r}, \boldsymbol{v}) = 2\Delta^*(\boldsymbol{r}, \boldsymbol{v})g(\omega, \boldsymbol{r}, \boldsymbol{v}). \tag{2}$$

Here $\boldsymbol{\Pi} = \boldsymbol{\nabla} + (2\pi \mathrm{i}/\Phi_0)\boldsymbol{A}$ is the gauge invariant gradient, $\boldsymbol{A}$ is the vector potential, Φ_0 is the flux quantum and $\boldsymbol{v} = \boldsymbol{v}(\boldsymbol{k}_\mathrm{F})$ is the Fermi velocity defined as $\boldsymbol{v}(\boldsymbol{k}) = \boldsymbol{\nabla}_k E(\boldsymbol{k})$, with $E(\boldsymbol{k})$ being the energy function of the electrons in the band; the Fermi wavevector $\boldsymbol{k}_\mathrm{F}$ can be found from the equation $E(\boldsymbol{k}) = E_\mathrm{F}$; $\omega = \pi T(2n + 1)$ with integer n is the Matsubara frequency, g and f are the normal and anomalous Green's function and $f^\dagger(\omega, \boldsymbol{r}, \boldsymbol{v}) = f^*(\omega, \boldsymbol{r}, -\boldsymbol{v})$. The normalization condition for the Green's functions is $g^2 + ff^\dagger = 1$.

The selfconsistency equations for the gap function and current density are

$$\Delta(\boldsymbol{r}, \boldsymbol{v}) = 2\pi N_0 T \sum_{\omega>0}^{\omega_\mathrm{D}} \int_\mathrm{FS} \mathrm{d}^2 k'_\mathrm{F} V(\boldsymbol{v}, \boldsymbol{v}')\rho(\boldsymbol{k}'_\mathrm{F}) f, \tag{3}$$

$$\boldsymbol{j} = 4\pi \mathrm{i}|e|N_0 T \sum_{\omega>0} \int_\mathrm{FS} \mathrm{d}^2 k_\mathrm{F} \rho(\boldsymbol{k}_\mathrm{F})\boldsymbol{v}g. \tag{4}$$

Here, $\int_\mathrm{FS}$ is the integral over the Fermi surface, ω_D is the cut-off frequency, N_0 is the total density of states for one spin at the Fermi surface in the normal state

$$N_0 = \int_\mathrm{FS} \frac{\mathrm{d}^2 k_\mathrm{F}}{(2\pi)^3} \frac{1}{|\boldsymbol{v}|}, \tag{5}$$

and $\rho(\boldsymbol{k}_\mathrm{F})$ is the angle resolved density of states at the Fermi surface:

$$\rho(\boldsymbol{k}_\mathrm{F}) = \frac{1}{(2\pi)^3 N_0} \frac{1}{|\boldsymbol{v}|}, \tag{6}$$

normalized so that

$$\int_\mathrm{FS} \mathrm{d}^2 k_\mathrm{F} \rho(\boldsymbol{k}_\mathrm{F}) = 1. \tag{7}$$

Density of states $N(\boldsymbol{r}, E)$ is defined as

$$N(\boldsymbol{r}, E) = N_0 \int_\mathrm{FS} \mathrm{d}^2 k_\mathrm{F} \,\mathrm{Re}\, g(\mathrm{i}\omega = E + \mathrm{i}\delta, \boldsymbol{r}, \boldsymbol{v})\rho(\boldsymbol{k}_\mathrm{F}). \tag{8}$$

We are interested in the low temperature zero-energy density of states (ZEDOS) $N(\boldsymbol{r}, E = 0)$. This is because in the limit of small temperatures, $T \longrightarrow 0$, the ratio of the specific heats in the superconducting state C_s and the normal state C_n is given by

$$\lim_{T\to 0} \frac{C_\mathrm{s}}{C_\mathrm{n}} = \frac{\overline{N(\boldsymbol{r}, E = 0)}}{N_0}. \tag{9}$$

Here $\overline{N(\boldsymbol{r}, E = 0)}$ is the spatially averaged ZEDOS in the superconducting state. In our calculation we set $T = T_\mathrm{c}/10$. Since ZEDOS and specific heat are proportional at low temperatures we use these two terms concurrently throughout the text. The numerical procedure for solving quasi-classical equations of superconductivity is described in [14]. Magnetic field is measured in units $\Phi_0/(2\pi R_0^2)$, where Φ_0 is the flux quantum, and $R_0 = 0.882\xi_0$ (ξ_0 is the BCS coherence length).

The angular dependence of ZEDOS is already studied numerically for some typical cases of nodal gap function: 3D d-wave, polar state and axial state [3]. The case of two-dimensional d-wave superconductors is well studied within the Doppler shift approximation, for the clean case [14–16], and also ZEDOS is studied by using the high field approximate solution of

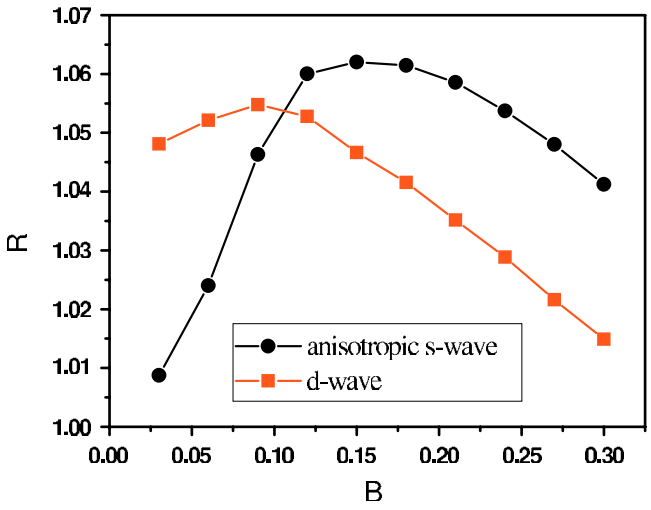

Figure 1. Ratio $R = N(E = 0, \varphi = 0)/N(E = 0, \varphi = \frac{\pi}{4})$ of minimum and maximum ZEDOS for fields rotating in the basal plane of the crystal. Full circles are for anisotropy parameter $a = 0.5$, while full squares are for the 2D d-wave superconductor ($a = 1$).

the Eilenberger equations [18–22]. The focus in that study was on the field dependence of ZEDOS for characteristic magnetic field directions. Just to recall, as one rotates the magnetic field from the gap node direction toward the gap maximum direction, ZEDOS increases in low field, while it decreases in fields near H_{c2}. In other words, the specific heat oscillation amplitude changes sign with increasing field. In this paper we compare the ZEDOS oscillation amplitude for nodal and nodeless superconductors in the limit of low fields. Along with the nodal gap structures already studied in [3], we also present results for some other typical cases known in the literature.

3. Nodal gap versus nodeless gap

In order to distinguish the nodal gap superconductor from the nodeless superconductor with a finite minimum gap, we examine the following model for the gap structure:

$$\Omega(\varphi, \theta) = \Omega_0(a)\sqrt{1 + a\cos 4\varphi} \tag{10}$$

with φ the polar angle and θ the azimuthal angle in polar coordinates. The parameter a measures the degree of anisotropy. For $a = 0$ the gap function is isotropic, while for $a = 1$ the gap function reduces to the two-dimensional (2D) version of $d_{x^2-y^2}$-wave superconductivity. We choose the prefactor $\Omega_0(a)$ so that the average of Ω^2 over the Fermi surface is unity, independent of a. ZEDOS is calculated for fields rotating in the basal plane with $\theta = \pi/2$. Only two field directions are of interest, B along the gap minimum ($\varphi = (2k + 1)\pi/4$), and B along the gap maximum ($\varphi = k\pi/2$). Here, k is integer. We performed the calculation for two anisotropy parameters: $a = 0.5$ and $a = 1$. In both cases, low field ZEDOS is always minimum when the magnetic field is oriented along the gap minimum (node) and vice versa.

In figure 1 the ratio $R = N(E = 0, \varphi = 0)/N(E = 0, \varphi = \frac{\pi}{4})$ of maximum and minimum ZEDOS, for a field rotating in the basal plane, is plotted for both anisotropy parameters. As is clear from figure 1, there is a striking difference in the low field dependence of ratio R for the nodal $a = 1$ and nodeless $a = 0.5$ superconducting gap. Namely, for the nodal gap case ($a = 1$) there is a finite amplitude ZEDOS oscillation ($R \neq 1$) towards $B \to 0$. This is contrasted with the nodeless gap case ($a = 0.5$) where R becomes unity at lower fields, showing a maximum at the intermediate field region $B_{\max}$. This means that the specific heat oscillation diminishes there. The field $B_{\max}$ comes from the physical reason that at $B < B_{\max}$

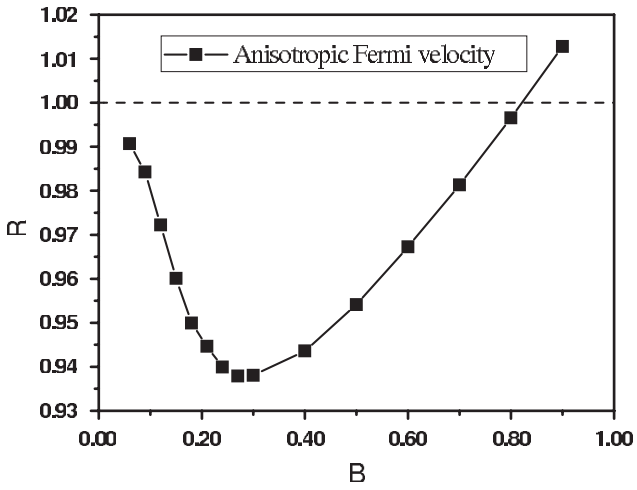

Figure 2. Ratio $R = N(E = 0, \varphi = 0)/N(E = 0, \varphi = \frac{\pi}{4})$ of minimum and maximum ZEDOS in the case of anisotropic Fermi velocity modelled by equation (11).

the spatial extension of the ZEDOS is confined to each vortex core region, yielding a more or less isotropic ZEDOS landscape. This ZEDOS feature does not cause the specific heat oscillation in this lower field. The spatial extension of the ZEDOS landscape depends on the size of the minimum gap because the gap acts as a potential for quasi-particles; that is, the zero-energy quasi-particles are strongly confined and localized near each core. Thus $B_{\max}$ signals the characteristic field where the localized zero-energy quasi-particles begin overlapping and tends to become smaller as the minimum gap decreases. Since in the nodal gap case the spatial extension of the ZEDOS is extended to infinity, $B_{\max}$ approaches zero, indicating that R stays constant towards smaller fields.

4. Anisotropic Fermi velocity

We analyse the other type of anisotropy. The superconducting gap is assumed to be isotropic, or to have the same value all over the Fermi surface, but the Fermi velocity itself is anisotropic. The amplitude of the Fermi velocity on the Fermi sphere is modelled as

$$v(\varphi, \theta) = v_0(b)(1 + b\cos 4\varphi). \tag{11}$$

The parameter b measures the degree of anisotropy. For convenience the prefactor $v_0(b)$ is chosen so that the density of states in the normal state is independent of b. Fourfold variation of the Fermi velocity in the basal plane is quite a simple model but will suffice for our purpose. Even in this hypothetical case with the isotropic gap and the anisotropic Fermi velocity, ZEDOS, and thus specific heat, depend on magnetic field direction. In figure 2, we plot the ratio R of minimum and maximum ZEDOS as a function of magnetic field. The anisotropy parameter $b = 0.5$ is used in the calculation. The ratio R between maximum and minimum ZEDOS is of the order of a few per cent. This is the same order of magnitude as in the above gap anisotropy cases. This is also the same order of magnitude as observed [11] in $LuNi_2B_2C$. This warns us that the effect of the Fermi surface structure on the specific heat oscillation cannot be neglected in intermediate fields. However, it is seen from figure 2 that extrapolation of the maximum/minimum ratio R to $B = 0$ gives $R = 1$, i.e. disappearance of specific heat oscillation. This is qualitatively the same behaviour as seen in the anisotropic gap case with a finite minimum gap, shown in figure 1. Physically this is due to the spatial extension of the zero-energy quasi-particle state. In the Fermi velocity anisotropy case ZEDOS

is confined to each core in a rather isotropic gap manner. Thus to induce the oscillation finite field is needed, above which, because of the overlapping of the zero-energy quasi-particles, ZEDOS begins to exhibit an oscillation.

It is also noticed that in the above $b > 0$ case $R < 1$, meaning that the fourfold oscillation pattern is maximally phase shifted by $\pi/4$ from the gap anisotropy cases with $R > 1$ in figure 1. Needless to say, the sign b is arbitrary for a given material, but it is physically plausible that $b > 0$ when $a > 0$ because in the angle-resolved DOS $N(\varphi) \propto 1/v(\varphi)$ the larger energy gap ($\varphi = 0$) coincides with the larger angle-resolved DOS. This is indeed the case in boro-carbides. Therefore, we can clearly distinguish the two anisotropy effects by measuring the angle-dependent specific heat to monitor both the oscillation amplitude and its phase.

5. Point node gap

In this section we consider the point node gap structure. Among several possible point node topologies we take up typical examples, the so-called axial state and 's + g' model. The former is known to be realized in the superfluid ^{3}He A phase and the latter is a candidate for boro-carbides [23]. We also consider the polar state with a line node for comparison.

5.1. Axial and polar gap function

The polar gap function has a horizontal line node in the crystal basal plane, while the axial gap function is characterized by two pointlike nodes at the poles of the Fermi sphere. In polar coordinates with φ and θ denoting polar and azimuthal angles, then the polar gap function is presented as

$$\Omega(\varphi, \theta) = \sqrt{3}\cos\theta, \tag{12}$$

and the axial gap function is presented as

$$\Omega(\varphi, \theta) = \sqrt{3/2}\sin\theta. \tag{13}$$

The low temperature ZEDOS for these two gap functions is studied in detail in [3]. By rotating the magnetic field in a plane that contains the c-axis, ZEDOS periodically changes. The ZEDOS maximum appears for the field oriented along the gap node, and the ZEDOS minimum appears when the magnetic field is directed along the gap maximum. Although the field dependence of ZEDOS has already been presented in [3], for the purpose of this paper we present these data in a slightly different form. Namely, we are interested in the amplitude of the ZEDOS oscillation as a function of B. Therefore, in figure 3 the field dependence of ratio $R = N(E = 0, \text{antinodal})/N(E = 0, \text{nodal})$ is shown. The low field ratio differs significantly for the axial and polar gap functions. The important point to notice is that in both cases the ratio R, in the limit of low fields, differs from unity. This means that there is a finite amplitude of ZEDOS oscillation as $H \longrightarrow 0$. This is in accord with the conclusion in the previous sections.

5.2. 's + g' model

It has been argued that the gap function in boro-carbides is a mixture of s-wave and g-wave superconductivity with aptly chosen weighting factors so that the pairing potential $\Omega(\varphi, \theta)$ does not change sign on the Fermi surface but has pointlike zeros:

$$\Omega(\varphi, \theta) = \sqrt{\frac{315}{379}}(1 - \sin^4\theta\cos 4\varphi). \tag{14}$$

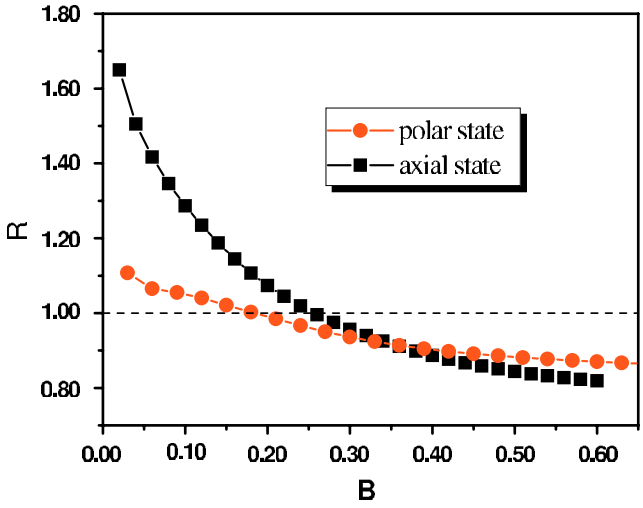

Figure 3. Ratio $R = N(E = 0, \text{antinodal})/N(E = 0, \text{nodal})$ as a function of magnetic induction for polar and axial gap functions.

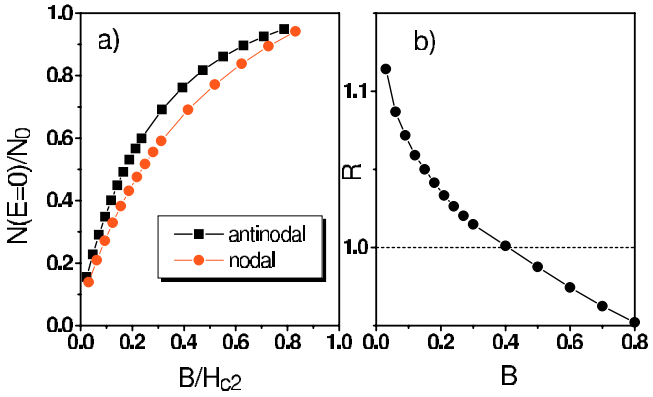

Figure 4. (a) Field dependence of ZEDOS for two field directions: nodal and antinodal when fields are rotated in the basal plane. (b) Ratio $R = N(E = 0, \text{antinodal})/N(E = 0, \text{nodal})$ as a function of magnetic induction for the 's + g' gap function.

As in previous examples of anisotropic pairing functions, we choose the Fermi surface as a sphere to see the effect of the gap structure on low temperature thermodynamics. As we have already shown, even the anisotropy of the Fermi surface alone can account for direction dependent specific heat. The effect of the Fermi surface disappears only in the limit of low fields. Having in mind that band structure in boro-carbides is far from being isotropic, this simple 's + g' gap function on the Fermi sphere may not be an appropriate model which can accurately estimate the amplitude of specific heat oscillation in boro-carbides, but we can gain a qualitative tendency in this case. In figure 4(a) the field dependence of low-temperature zero-energy DOS is shown for nodal and antinodal field directions. We define the antinodal direction as a direction in the basal plane with maximum value of superconducting gap. Magnetic induction B is scaled with H_{c2}(antinodal) and H_{c2}(nodal) respectively. Note that $H_{c2}(\text{antinodal}) > H_{c2}(\text{nodal})$. As one may already anticipate, the difference between the maximum ZEDOS (field along the antinodal direction) and the minimum ZEDOS (field along the nodal direction) remains finite in low fields. Thus their ratio $N(E = 0, \text{antinodal})/N(E = 0, \text{nodal}) \neq 1$. This is shown in figure 4(b). Noteworthy is the comparison with the gap structure of the axial state $\Omega(\varphi, \theta) = \sqrt{3/2}\sin\theta$. Both the axial state and the 's + g' model have point-like nodes, while their field dependence of ZEDOS is different. The $\gamma(B)$ behaviour as a function of B is not governed only by the gap node

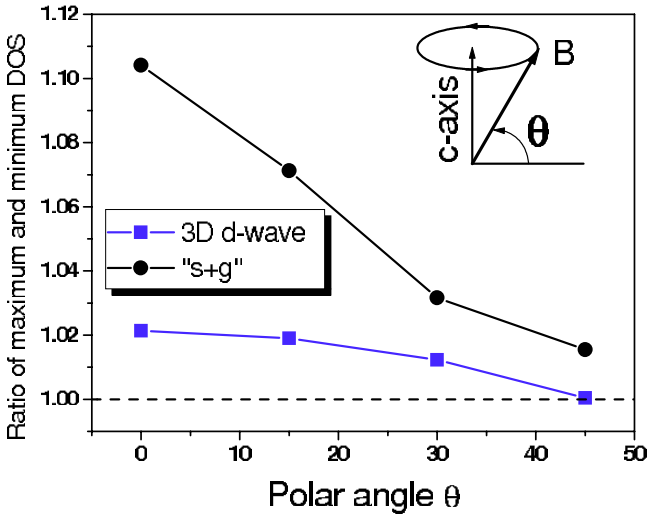

Figure 5. Ratio of maximum and minimum DOS as field rotates conically around the c-axis for fixed polar angle θ. The relative position of magnetic field B and crystal c-axis is shown in the inset of the figure.

topology, point-like or line-like nodes. It is not unique for all types of gap structures with point-like (or line-like) nodes. It rather reflects the gap value on average, and it is rather sensitive to the functional form of the gap function in the vicinity of the node.

6. Discussions on the specific heat experiments

In this section we discuss the angle dependent specific heat experiments on three materials, $LuNi_2B_2C$, $CeCoIn_5$ and Sr_2RuO_4, in the light of the present calculations.

6.1. Boro-carbides

Park *et al* [11] measure the angle-dependent $\gamma(B)$ for $LuNi_2B_2C$ and detect the fourfold oscillations in various fields, identifying that the gap minimum is located in the [100] direction of the tetragonal crystal because the oscillation maximum is in the [110] direction. This identification is supported by our present result. The oscillation amplitude becomes smaller as B decreases. However, it is rather difficult to judge whether the gap has a node or a finite minimum gap from their experiment, where the detailed low field data are lacking. In connection with other experiments which suggest a strong anisotropic gap [24] or s point node gap [25] in this system, it is interesting to extend their measurement to lower field to determine the precise gap structure.

Izawa *et al* [25] show in their angle-dependent thermal conductivity measurement that (1) in the similar oscillation pattern the maximum appears in [110], coinciding with that in Park *et al*, and (2) the oscillation amplitude diminishes when the field rotates conically out of the basal plane. For the polar angle $\theta > \pi/4$ it almost vanishes. They conclude a point node gap located along the [100] direction. This assertion is based on a theoretical calculation [23] of angle dependence of thermal conductivity. It may be informative in this connection to show our result: we have also performed the calculation when the field rotates conically to check how the oscillation amplitude varies as a function of the polar angle θ as shown in figure 5. It is found that it decreases quickly as θ increases from zero for both the vertical line node and the 's + g' point node cases. In the vertical line node case the oscillation amplitude decreases rapidly as θ increases, but it remains finite even for $\theta = 45°$. In the 's + g' point node case the

oscillation amplitude decreases gradually up to $\theta \sim 30°$, then becomes diminishing for larger angles. Because of these reasons it is difficult to distinguish these two cases by a conical field rotation of specific heat experiment.

6.2. $CeCoIn_5$

Aoki *et al* [12] perform the angle dependent specific heat experiment in this system, observing a substantial oscillation amplitude when rotating the field within the basal plane of the tetragonal symmetry crystal. In the oscillation pattern the maximum occurs for the [110] direction. This suggests the d_{xy} gap function because the oscillation amplitude stays constant towards the lowest fields. This conclusion appears to be inconsistent with the angle-dependent thermal conductivity experiment by Izawa *et al* [26], who conclude the $d_{x^2-y^2}$ gap function. Note, however, that their data themselves exhibit the oscillation maximum for the [110] direction, consistent with Aoki *et al* [12].

6.3. Sr_2RuO_4

According to Deguchi *et al* [13], who measure the angle-dependent specific heat on this system by rotating the field within the basal plane of the tetragonal crystal, the fourfold oscillation amplitude decreases below a threshold field ∼0.3 T and changes its sign near $B_{c2} \sim 1.5$ T. The existence of the threshold field is in accord with our calculation, where the gap structure has a finite minimum gap, definitely excluding the vertical line node in the so-called main γ band. (We cannot say anything about the possible horizontal line node [27].) An interesting point in this system is the fact that we know accurately the Fermi velocity anisotropy in the γ band, where the larger Fermi velocity is directed to [110]. Since the observed oscillation maximum occurs along [110], the experiment unambiguously excludes the oscillation due to the Fermi velocity anisotropy. Combining these two facts, we conclude that there exists an anisotropic gap structure with a finite minimum in the basal plane of the main γ band in Sr_2RuO_4. We cannot commit ourselves on further conclusions concerning the minor α and β bands or the horizontal line node based on the existing data by Deguchi *et al* [13].

7. Summary and conclusion

In this paper, we have calculated the zero-energy density of states in the mixed state at low temperature by employing quasi-classical Eilenberger formalism, which is valid for a wide variety of superconductors. We have focused on the angle dependence of the zero-energy density of states, which is directly measured through a specific heat experiment as the Sommerfeld coefficient, for superconductors with both nodal and nodeless gap structures.

We have demonstrated that the specific heat angular dependence provides useful information concerning the gap structure, namely, the position of the node or the gap minimum on the Fermi surface and also the existence or non-existence of the gap node. Furthermore, we give information to distinguish two sources of the anisotropy, either due to the gap itself or due to the Fermi velocity of the band structure. These proposed methods, we believe, add yet another dimension to firmly establish the gap structure.

A few examples studied here do not exhaust all possibilities for superconducting gap function. Neither can all kinds of different Fermi surface structures be covered. Nevertheless, from the comparison of field dependence of ZEDOS in (a) nodal and (b) fully gapped anisotropic superconductors, one can conjecture a behaviour that is common for each group of superconductors. In nodal superconductors the specific heat oscillation amplitude persists

down to very low fields. In contrast to this behaviour, for fully gapped superconductors, as one decreases magnetic field the oscillation amplitude gradually diminishes. To remind the reader again, only low temperature specific heat is discussed here.

Acknowledgments

We are grateful for useful discussions and communication with Y Matsuda, T Sakakibara, K Izawa, J Sonier, K Deguchi, Y Maeno, A Junod and M Salamon.

References

[1] Volovik G E 1993 *JETP Lett.* **58** 469
[2] Ichioka M, Hasegawa A and Machida K 1999 *Phys. Rev.* B **59** 8902
Ichioka M, Hasegawa A and Machida K 1999 *Phys. Rev.* B **59** 184
[3] Miranović P, Nakai N, Ichioka M and Machida K 2003 *Phys. Rev.* B **68** 052501
[4] Sonier J E, Hundley M F, Thompson J D and Brill J W 1999 *Phys. Rev. Lett.* **82** 4914
[5] Ramirez A P 1996 *Phys. Lett.* A **211** 59
[6] Guritanu V, Goldacker W, Bouquet F, Wang Y, Lortz R, Goll G and Junod A 2005 *Phys. Rev.* B **70** 184526
[7] Hedo M, Inada Y, Yamamoto E, Haga Y, Onuki Y, Aoki Y, Matsuda T D, Sato H and Takahashi S 1998 *J. Phys. Soc. Japan* **67** 272
[8] Nohara M, Isshiki M, Sakai F and Takagi H 1999 *J. Phys. Soc. Japan* **68** 1078
[9] Mirmelstein A, Junod A, Walker E, Revaz B, Genoud J Y and Triscon G 1997 *J. Supercond.* **10** 527
[10] Nakai N, Miranović P, Ichioka M and Machida K 2004 *Phys. Rev.* B **70** 100503
[11] Park T, Salamon M B, Choi E M, Kim H J and Lee S-I 2003 *Phys. Rev. Lett.* **90** 177001
Park T, Chia E E M, Salamon M B, Bauer E D, Vekhter I, Thompson J D, Choi E M, Kim H J, Lee S-I and Canfield P C 2004 *Phys. Rev. Lett.* **92** 237002
[12] Aoki H, Sakakibara T, Shishido H, Settai R, Onuki Y, Miranović P and Machida K 2004 *J. Phys.: Condens. Matter* **16** L13
[13] Deguchi K, Mao Z Q, Yaguchi H and Maeno Y 2004 *Phys. Rev. Lett.* **92** 047002 (*Preprint* cond-mat/0404070)
[14] Miranović P, Ichioka M and Machida K 2004 *Phys. Rev.* B **70** 104510
[15] Vekhter I, Hirschfeld P J, Carbotte J P and Nicol E J 1999 *Phys. Rev.* B **59** R9023
[16] Schachinger E and Carbotte J P 1999 *Phys. Rev.* B **60** 12400
[17] Hirschfeld P J 1998 *J. Korean Phys. Soc.* **33** 485
[18] Dahm T, Graser S, Iniotakis C and Schopohl N 2002 *Phys. Rev.* B **66** 144515
[19] Kusunose H 2004 *J. Phys. Soc. Japan* **73** 2512
[20] Kusunose H 2004 *Phys. Rev.* B **70** 054509
[21] Udagawa M, Yanase Y and Ogata M 2005 *Phys. Rev.* B **71** 024511
[22] Udagawa M, Yanase Y and Ogata M 2004 *Phys. Rev.* B **70** 184515
[23] Thalmeier P and Maki K 2003 *Acta Phys. Pol.* B **34** 557
Maki K, Won H and Haas S 2004 *Phys. Rev.* B **69** 012502
[24] Watanabe T, Nohara M, Hanaguri T and Takagi H 2004 *Phys. Rev. Lett.* **92** 147002
[25] Izawa K, Kamata K, Nakajima Y, Matsuda Y, Watanabe T, Nohara M, Takagi H, Thalmeier P and Maki K 2002 *Phys. Rev. Lett.* **89** 137006
[26] Izawa K, Yamaguchi H, Matsuda Y, Shishido H, Settai R and Onuki Y 2001 *Phys. Rev. Lett.* **87** 057002
[27] Hasegawa Y, Machida K and Ozaki M 2000 *J. Phys. Soc. Japan* **69** 336
Hasegawa Y and Yakiyama M 2003 *J. Phys. Soc. Japan* **72** 1318